Chinese Journal of
POLYMER SCIENCE

RESEARCH ARTICLE

https://doi.org/10.1007/s10118-026-3654-1
Chinese J. Polym. Sci.

Transparent UV-cured Phosphorus/Nitrogen Hybrid Coating for Simultaneously Enhancing Flame Retardancy and Surface Hardness of Polycarbonate

Jing Gao[a], Liang Chen[a], Liang-Yuan Qi[a], Su-Hong Li[a], Yuan Hu[a], Xin Wang[a], Lian-Min Ji[c], Ying-Jian Wang[b*], and Wei-Yi Xing[a*]

[a] *State Key Laboratory of Fire Science, University of Science and Technology of China, Hefei 230026, China*
[b] *School of Intelligent Engineering and Automation, Beijing University of Posts and Telecommunications, Beijing 102206, China*
[c] *Key Laboratory of Green and High-end Utilization of Salt Lake Resources, Qinghai Institute of Salt Lakes, Chinese Academy of Sciences, Qinghai 810008, China*

Electronic Supplementary Information

Abstract The flame-retardant monomer PG (P) was synthesized from diethylphosphinic acid and glycidyl methacrylate (GMA). Simultaneously, the phosphorus-containing flame-retardant monomer, TAEP (T), was synthesized from phosphorus oxychloride and 2-hydroxyethyl acrylate. A 50 μm thick transparent UV-cured coating, designated MAAR-P_8T_4, was successfully constructed on 0.5 mm thick polycarbonate (PC) films by blending PG and TAEP with melamine acrylate resin (MAAR). The fabricated coating demonstrated a high transmittance of 91.9% in the visible-light spectrum. The incorporation of monofunctional PG effectively regulated the system viscosity and mitigated curing shrinkage stress. Furthermore, the synergistic action of phosphorus in different valence states and nitrogen from MAAR imparted a dual gas-phase-condensed phase flame-retardant mechanism to the coating, enabling the PC substrate to attain a V-0 rating in the UL-94 vertical burning test. This research indicates that the MAAR-P_8T_4 coating engineered *via* molecular design and component optimization concurrently overcomes the limitations of PC, namely its low surface hardness and inherent flammability. A straightforward and efficient preparation strategy provides a practical approach for transparent flame-retardant coatings for electronic and electrical applications.

Keywords Synergistic flame retardant system; UV-curable coatings; Transparent coating; Flame retardancy; Polycarbonate

Citation: Gao, J.; Chen, L.; Qi, L. Y.; Li, S. H.; Hu, Y.; Wang, X.; Ji, L. M.; Wang, Y. J.; Xing, W. Y. Transparent UV-cured phosphorus/nitrogen hybrid coating for simultaneously enhancing flame retardancy and surface hardness of polycarbonate. *Chinese J. Polym. Sci.* https://doi.org/10.1007/s10118-026-3654-1

INTRODUCTION

Polycarbonate (PC), a high-performance thermoplastic engineering polymer, is considered indispensable across numerous industrial sectors owing to its exceptional comprehensive properties and is extensively utilized in fields such as electrical and electronic appliances, automotive manufacturing, and safety protection.[1,2] Its principal merit is derived from its simultaneous possession of superior impact toughness, outstanding optical transparency, and favorable thermal stability. These distinctive strengths make PC an irreplaceable material in scenarios demanding high transparency coupled with high impact resistance.[3–5] Nevertheless, under unmodified conditions, PC is associated with a notable hazard of melting and dripping during combustion, potentially igniting other combustible substances.[6–8] This intrinsic combustion characteristic severely constrains its application in critical areas, where fire safety requirements are extremely rigorous. Consequently, the flame-retardant modification of PC, while preserving its inherent advantages, is endowed with both pressing engineering significance and substantial research value.

Flame-retardant modification of PC is primarily achieved through the following three approaches: The first method is melt blending. A novel ladder-like silsesquioxane developed by Wu *et al*. was utilized to prepare PC composites with excellent flame retardancy.[9] However, owing to issues concerning the dispersion and compatibility of the additive flame retardants within the polymer matrix, the transparency and mechanical properties of PC are often compromised, thereby limiting its application in high-end fields that require both high transparency and superior mechanical performance. The second method involves reactive copolymerization. The flame-retardant polycarbonate synthesized by Liu *et al*. was designated PC-SDP_n.[10] Given the stringent requirements for selecting flame retardants, this becomes a major constraint in broadening the application of flame-retardant PC. The third method is the surface treatment. A transparent flame-retardant coating developed by Zhang *et al*. was demonstrated to

* Corresponding authors, E-mail: wangyingjian@bupt.edu.cn (Y.J.W.)
E-mail: xingwy@ustc.edu.cn (W.Y.X.)
Received January 5, 2026; Accepted March 10, 2026; Published online July 2, 2026

© Chinese Chemical Society
Institute of Chemistry, Chinese Academy of Sciences

simultaneously enhance the surface hardness and flame retardancy of PC simultaneously.[11] Similarly, a transparent flame-retardant coating prepared by Feng *et al.* was reported to improve both the flame and scratch resistance of PC.[12] By applying a functional coating onto the PC surface, its inherent excellent properties can be preserved, thereby resolving the inherent conflict between flame retardancy and the demand for high transparency and mechanical performance. However, when applied to a 0.5 mm-thick polycarbonate film, both coatings caused deformation of the film during curing.

In previous studies, flame retardants employed for polycarbonates have primarily included halogen-,[13] sulfur-,[14] phosphorus-,[15] and silicon-based types.[16] Although halogen-based flame retardants demonstrate outstanding efficiency, their application has been restricted or phased out in many regions, owing to potential environmental and health concerns.[17] In contrast, phosphorus-based compounds, which are characterized by their high flame-retardant effectiveness, are regarded as promising alternatives to replace harmful halogenated flame retardants in flame-retardant polymer materials.[18–22] Phosphorus-based flame retardants can be classified into two main categories: inorganic and organic. For instance, BP@MIL-53, synthesized *via* a hydrothermal method by Qian *et al*., was used to fabricate PC composites with excellent flame retardancy and thermal stability, although its optical transparency was compromised.[23] In another approach, a film containing phosphorus and silicon was deposited onto a PC using atmospheric pressure plasma technology by Hilt *et al*., leading to a successful enhancement of its flame-retardant performance.[24] Furthermore, a phosphorus-containing monomer synthesized from cardanol derived by Li *et al*. was copolymerized with commercial acrylic monomers, resulting in the preparation of an intumescent flame-retardant coating exhibiting phosphorus-nitrogen synergy.[25] This coating was proven to simultaneously improve both the flame resistance and scratch resistance of the PC. Consequently, phosphorus-based flame retardants are considered to have significant potential for the construction of high-performance multifunctional coatings.

In this study, two flame-retardant UV-curable monomers, PG and TAEP, were synthesized. Subsequently, these monomers were formulated with melamine acrylate resin (MAAR) to fabricate a transparent UV-curable coating on 0.5 mm-thick PC films. The resultant coating, with a controlled thickness of 50 μm, exhibited an average visible-light transmittance of 91.9%. Owing to the synergistic effect between phosphorus-containing flame-retardant monomers and MAAR, the MAAR-P_8T_4 formulation achieved an optimal balance between flame-retardant performance and high transparency performance. Notably, the coated film not only significantly enhanced the hardness of the PC substrate from 2B to 3H on the pencil hardness scale but also attained a V-0 rating in the UL-94 vertical burning test. This study provides an economical and efficient strategy for the production of high-transparency PC films with superior flame retardancy.

EXPERIMENTAL

Materials

2-Hydroxyethyl acrylate (HEA), diethylphosphinic acid, 4-Methoxyphenol (MEHQ), phosphorus (V) oxychloride ($POCl_3$), and glycidyl methacrylate (GMA) were purchased from Aladdin Industrial Company (China). Triethylamine (TEA), diethyl ether, and toluene were obtained from Sinopharm Chemical Reagent Co., Ltd., (Shanghai, China). Melamine acrylate resin (MAAR) was obtained from Jiangsu Sanmu Chemicals Co., Ltd., (Jiangsu, China). 2,4,6-Trimethylbenzoyldiphenyl phosphine oxide (TPO) used as photoinitiator was obtained from Curease Chemical Group Co., Ltd., (Shanghai, China). Polycarbonate films (0.5 mm thick) were supplied by Shanghai Polyshine Group Co., Ltd., (Shanghai, China). All the chemical reagents were used directly without further purification.

Synthesis of Phosphorus-containing UV-curable Monomers

The synthesis of TAEP (Fig. 1a) was based on a previous study, with modifications.[26] A solution containing 0.3 mol (34.84 g) of HEA and 0.3 mol (30.36 g) of TEA in 100 mL of anhydrous diethyl ether was mechanically stirred in a 250 mL three-necked

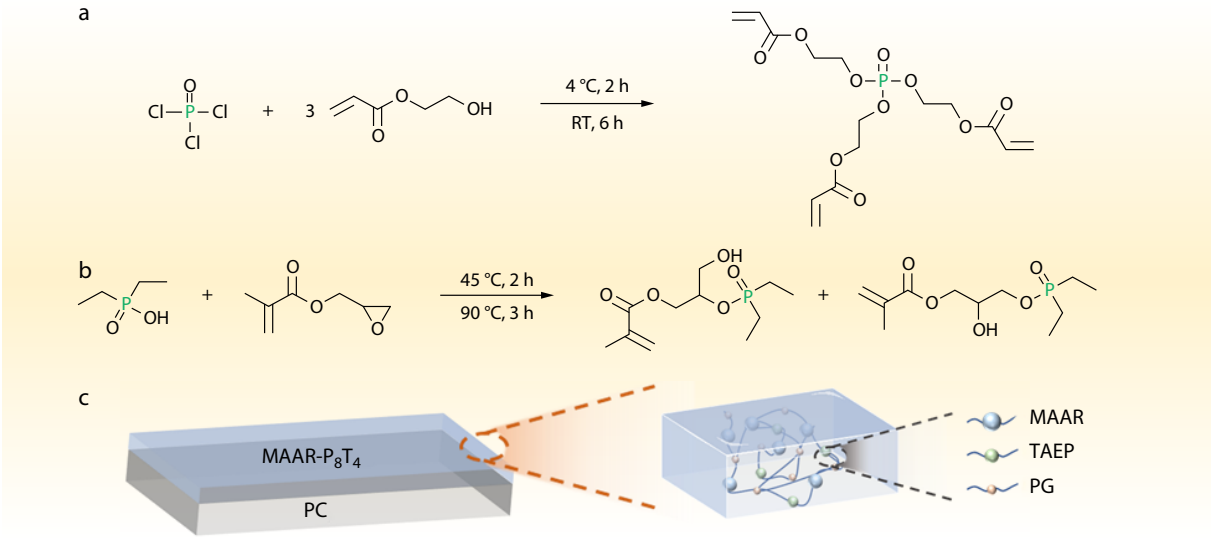

Fig. 1 (a) Synthesis of TAEP; (b) Synthesis of PG; (c) Curing mechanism of MAAR-P_mT_n.

https://doi.org/10.1007/s10118-026-3654-1

flask. Under ice bath cooling, 0.1 mol (15.33 g) of $POCl_3$ was added dropwise over 30 min. The reaction mixture was then stirred at ambient temperature for 8 h. After the reaction was complete, the byproduct salts were removed by filtration, and the solvent was eliminated *via* rotary evaporation, yielding TAEP as a pale-yellow transparent liquid.

The synthesis of PG, as outlined in Fig. 1(b), proceeds as follows. Diethylphosphinic acid (0.1 mol, 12.21 g) and 0.1% MEHQ were dissolved in toluene (100 mL) in a 250 mL three-neck flask under magnetic stirring. GMA (0.1 mol, 14.21 g) was added dropwise over 30 min at 45 °C. Subsequently, the temperature was increased to 90 °C for a 3 h reaction period. Upon completion, the solvent was removed by rotary evaporation, yielding PG as a colorless liquid.

Preparation of UV-curable Coatings

MAAR, PG, TAEP, and the photoinitiator (TPO) were precisely weighed according to the ratios specified in Table 1 and homogenized under vacuum. This procedure afforded the UV-curable coating MAAR-P_mT_n (where *m* and *n* denote the mass fractions of PG and TAEP, respectively). The resulting coating was applied to PC films at a uniform thickness of 50 μm. Following the deposition, the samples were maintained horizontally under light-shielded conditions to permit spontaneous leveling. Subsequently, the films were radiation-cured using an 80 W/cm^2 UV lamp. The curing mechanism is illustrated in Fig. 1(c).

Table 1 Preparation of UV-curable coating MAAR-P_mT_n.

Sample	m_{PG} (g)	m_{TAEP} (g)	m_{MAAR} (g)	TPO (%)
MAAR-P_{12}	12	0	6	3
MAAR-P_6T_6	6	6	6	3
MAAR-P_8T_4	8	4	6	3
MAAR-P_6T_3	6	3	6	3
MAAR-P_9T_3	9	3	6	3

Instrumentation and Characterization

Instrumentation and characterization methodologies employed in this work are detailed in the electronic supplementary information (ESI).

RESULTS AND DISCUSSION

Structural Characterization of TAEP and PG

The chemical structures of TAEP and PG were characterized using Fourier transform infrared (FTIR) spectrometry, liquid chromatography-mass spectrometry (LC-MS), and nuclear magnetic resonance (NMR) spectroscopy. In Fig. 2(a), the three sets of peaks at δ=5.88–6.48 ppm corresponded to the alkenyl protons (a + b + c) of TAEP, while the signal at δ=4.3–4.4 ppm corresponded to its methylene protons (d + e).[26] Fig. 2(b) shows the signal at δ=−1.5 ppm corresponded to the phosphorus atom in TAEP. As demonstrated in Fig. 2(e), the signal of PG appears at δ=64.3 ppm corresponded to the phosphorus atom in PG. The LC-MS data (Fig. 2d) confirmed the successful synthesis of PG. The successful synthesis of TAEP is further evidenced by the appearance of the P—O stretch at 970 cm^{-1} and disappearance of the P—Cl vibration at 590 cm^{-1} in the FTIR spectra (Fig. 2c).[27,28] Similarly, the synthesis of PG was verified by the emergence of the —OH band at 3340 cm^{-1} concomitant with the disappearance of the C—O—C absorption at 1246 cm^{-1} (Fig. 2f).[29]

Physical Properties of MAAR-P_mT_n

The optical properties of the PC substrates coated with MAAR-

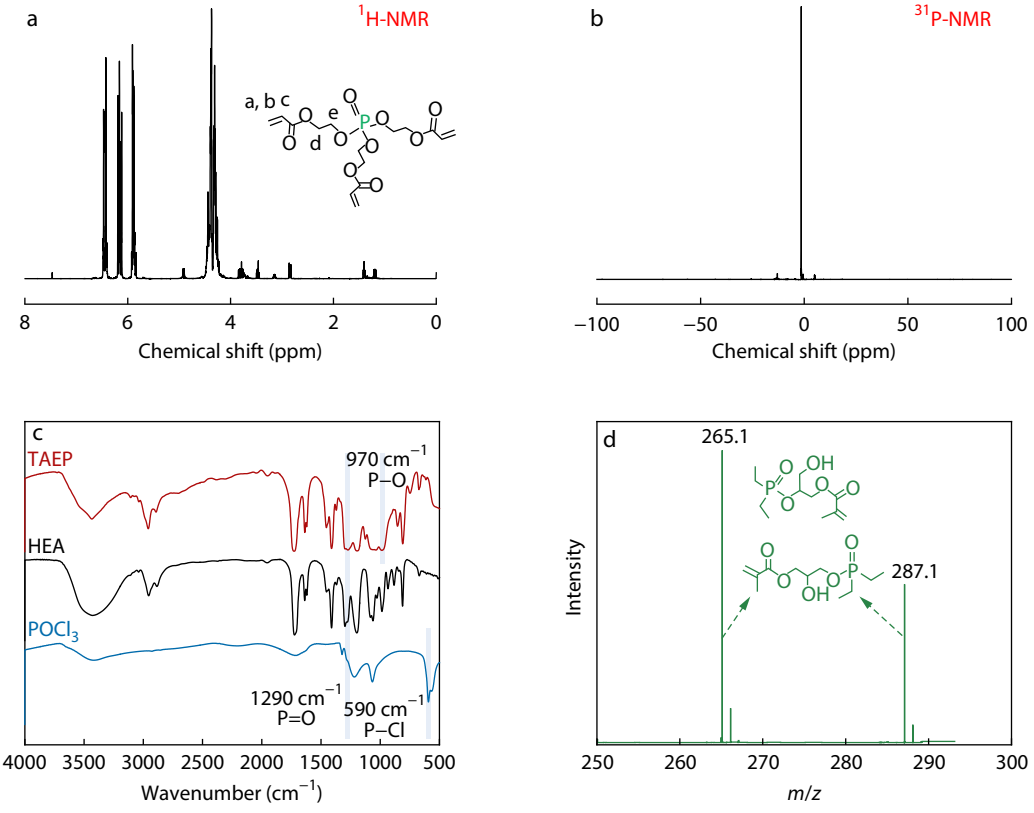

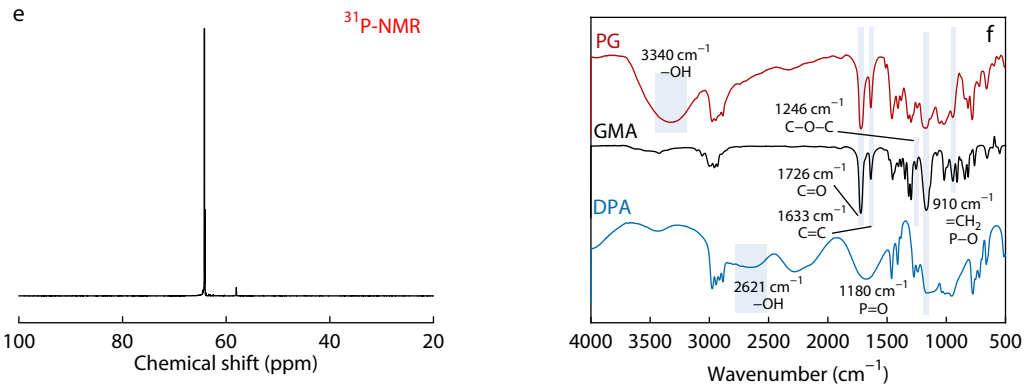

Fig. 2 (a) ^{1}H-NMR spectrum of TAEP; (b) ^{31}P-NMR spectrum of TAEP; (c) FTIR spectra of TAEP, HEA and $POCl_3$; (d) LC-MS spectrum of PG; (e) ^{31}P-NMR spectrum of PG; (f) FTIR spectra of PG, GMA and DPA.

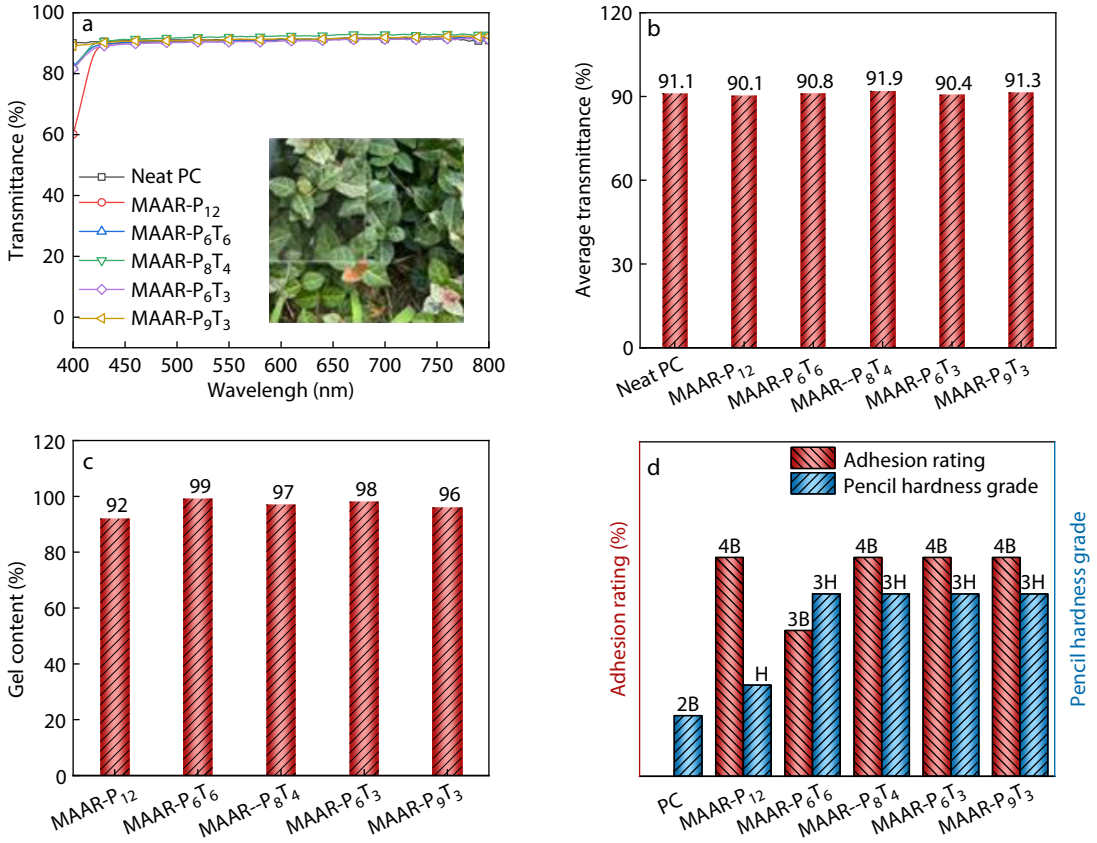

Fig. 3 Transmittance spectra of samples in the visible spectrum: (a) Original transmittance spectra; (b) Averaged transmittance spectra. (c) Gel content of coatings; (d) Adhesion rating and pencil hardness grade of samples.

P_mT_n were characterized by measuring their transmittance in the visible spectrum. The transmittance spectra presented in Figs. 3(a) and 3(b) demonstrate that the coated PC films maintain light transmission above 88% throughout the 400–800 nm wavelength range. As shown in Fig. S1 (in ESI), the average haze of all the PC samples coated with MAAR-P_mT_n was below 10%. This result confirms the exceptional optical transparency of the MAAR-P_mT_n coating system when applied to the PC substrates.

The gel content, defined as the mass ratio of the sample after the extraction and drying procedures to the original mass, serves as an indirect indicator of the cross-linking network density within the material and the structural compactness of the coating. To determine this parameter, the MAAR-P_mT_n coatings were subjected to continuous extraction in a Soxhlet apparatus, using toluene as the extraction solvent, at 130 °C for 24 h. Following extraction, the samples were thoroughly dried in a vacuum oven until constant mass was achieved, with the resultant data compiled in Fig. 3(c). Analysis of the results revealed an inverse correlation between gel content and increasing mass fraction of PG in the coating formulation. This phenomenon is ascribed to the lower functionality of PG relative to both TAEP and MAAR, which consequently limits

the development of crosslinked networks.[30]

Adhesion testing conducted per ASTM D3359-23 methodology showed that MAAR-P_6T_6 exhibited an adhesion rating of 3 B, while all other MAAR-P_mT_n coatings attained a superior 4B rating. The pencil hardness of the MAAR-P_mT_n coatings was evaluated according to the GB/T 6739—2022 standards, and the results are shown in Fig. 3(d). The analysis revealed that the unmodified PC films exhibited a pencil hardness grade of 2B. Notably, all MAAR-P_mT_n coated samples demonstrated significantly enhanced surface hardness, achieving a grade of 3H, with the exception of MAAR-P_{12}, which possesses a grade of H. This improvement in physical properties is attributed to the increased crosslinking density within the coating matrix, which directly correlates with the higher pencil hardness ratings.[31] These findings are consistent with the gel content data presented in the preceding section, thereby validating the structure-property relationships within this coating system.

Thermal Stability of Coatings

Thermogravimetric analysis (TGA) was employed to investigate the thermal degradation and thermo-oxidative behavior of the coatings under nitrogen and air atmospheres. Fig. 4 presents the TGA and derivative thermogravimetric (DTG) curves for the MAAR-P_mT_n specimens in both nitrogen and air environments. The key thermal stability parameters extracted from these analyses, including the 5% mass loss temperature ($T_{5\%}$), temperature at the maximum mass loss rate (T_{max}), maximum mass loss rate (R_{max}), and char yield (CY) at 800 °C, are summarized in Table 2.[32,33] Under air atmosphere, MAAR-P_9T_3 exhibited the lowest $T_{5\%}$ at 196 °C, indicative of the onset of premature thermal decomposition.[34,35] In contrast, MAAR-P_6T_6 exhibited the highest $T_{5\%}$ value at 289 °C. The DTG analysis further revealed that TAEP incorporation significantly reduced the decomposition rate during the primary pyrolysis stage of MAAR-P_{12}. Critically, T_{max} of MAAR-P_8T_4 increased by approximately 36 °C compared to that of MAAR-P_{12}. Char yield analysis at 800 °C demonstrated a positive correlation between the TAEP content and residual char formation, with CY values increasing as the TAEP mass content increased. Under nitrogen atmosphere, MAAR-P_{12}

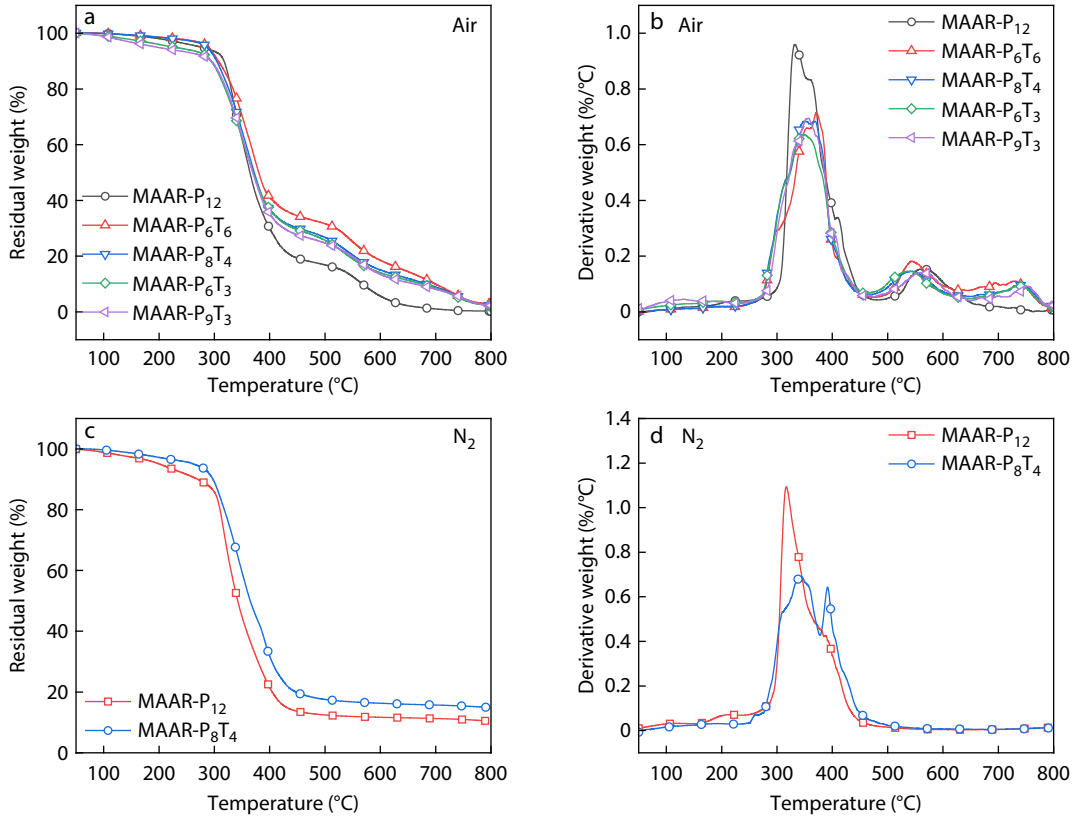

Fig. 4 (a) TG curves, (b) DTG curves of MAAR-P_mT_n in air; (c) TG curves, (d) DTG curves of MAAR-P_mT_n in nitrogen.

Table 2 Data related to thermogravimetric tests.

Sample	$T_{5\%}$ (°C)		T_{max} (°C)		R_{max} (%/°C)		CY (%)	
	Air	N_2	Air	N_2	Air	N_2	Air	N_2
MAAR-P_{12}	276	201	332	317	0.960	1.096	0.2	10.5
MAAR-P_6T_6	289	–	371	–	0.714	–	2.8	–
MAAR-P_8T_4	287	263	368	345	0.684	0.689	2.3	15.0
MAAR-P_6T_3	227	–	348	–	0.637	–	2.3	–
MAAR-P_9T_3	196	–	357	–	0.695	–	2.3	–

https://doi.org/10.1007/s10118-026-3654-1

and MAAR-P_8T_4 achieved char yields of 10.5% and 15.0%, respectively. This phenomenon is primarily attributable to the contrasting pyrolysis pathways of the components: TAEP exhibits a pronounced char-forming tendency during thermal decomposition, whereas PG predominantly undergoes gas-phase fragmentation with a significantly weaker char retention capability.[36,37] During pyrolysis, the TAEP and PG components generate phosphate derivatives that catalyze matrix dehydration and char formation. Simultaneously, MAAR acts as a gas source, releasing volatiles that facilitate char layer expansion.[38] This char layer effectively impedes oxygen diffusion and heat transfer.[39] The phosphorus-nitrogen synergistic effect was identified as the critical mechanism that enabled the formation of a char layer, thereby significantly enhancing the thermal stability of the coatings.

Flame Retardancy of Coatings

Microscale combustion calorimetry (MCC) was employed to analyze the combustion behavior of the MAAR-P_mT_n coatings, yielding critical parameters including the heat release rate (HRR), peak heat release rate (pHRR), and total heat release (THR). As shown in Fig. 5, both the THR and pHRR values were significantly reduced upon TAEP incorporation. Specifically, MAAR-P8T4 achieved 19.3% and 28.4% decreases in THR and pHRR, respectively, compared with MAAR-P12, attributable to the synergistic interaction between TAEP and PG. During pyrolysis, the TAEP and PG components generate phosphate compounds that catalyze matrix dehydration and carbonization, while the gas-source MAAR component releases pyrolytic gases to expand the char layer.[40,41] This expanded char structure effectively hindered oxygen ingress and heat transfer, a mechanism fully consistent with TGA.

The combustion behavior of PC and MAAR-P_mT_n-coated PC was systematically evaluated by the limiting oxygen index (LOI) and UL-94 vertical burning tests. As shown in Fig. 5(d), distinct behavioral variations emerged during UL-94 testing: PC, MAAR-P_{12}, and MAAR-P_9T_3 exhibited severe melt dripping that ignited the underlying absorbent cotton, whereas MAAR-P_6T_3 produced non-igniting droplets. Notably, MAAR-P_6T_6 suppressed dripping entirely but demonstrated a prolonged after-flame duration (41 s), whereas MAAR-P_8T_4 achieved the optimal V-0 rating. Concurrent LOI tests demonstrated that MAAR-P_8T_4 significantly enhanced the LOI value of PC from 22% to 27%.

Flame Retardant Mechanism

The graphitization degree of the residual char was quantitatively characterized *via* Raman spectroscopy, as enhanced graphitic ordering typically correlates with superior oxidation resistance and mechanical strength, thereby providing more effective protective effects for PC substrates.[42] Spectral analysis (Figs. 6a–6c) reveals two distinct characteristic bands at approximately 1590 cm^{-1} (G band) and 1350 cm^{-1} (D band) across all samples.[43,44] The intensity ratio of the D band to the G band area (I_D/I_G) serves as a critical metric for evaluating residual char ordering, where lower ratios indicate higher graphitization degrees.[45] Notably, MAAR-P_8T_4 exhibits a reduced I_D/I_G value of 2.58 compares to 2.66 for MAAR-P_{12}. This decrease conclusively demonstrates the

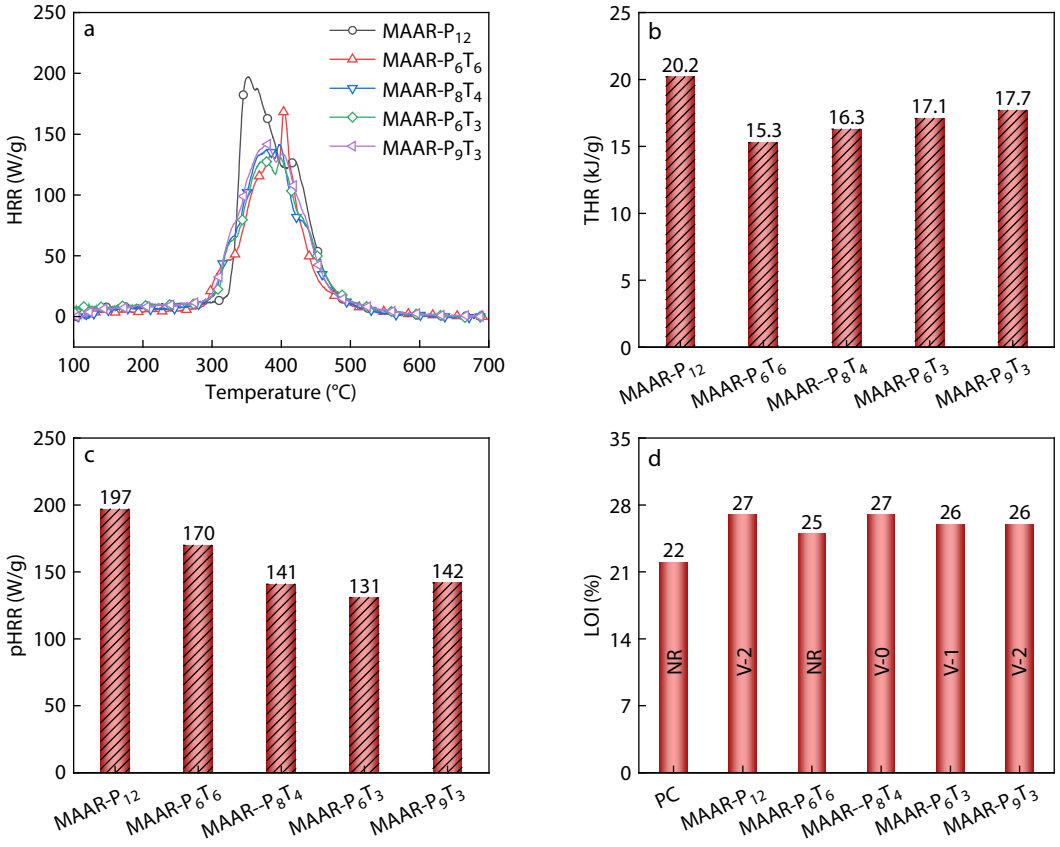

Fig. 5 (a) HRR curves, (b) THR values, (c) pHRR values, and (d) LOI values of the samples.

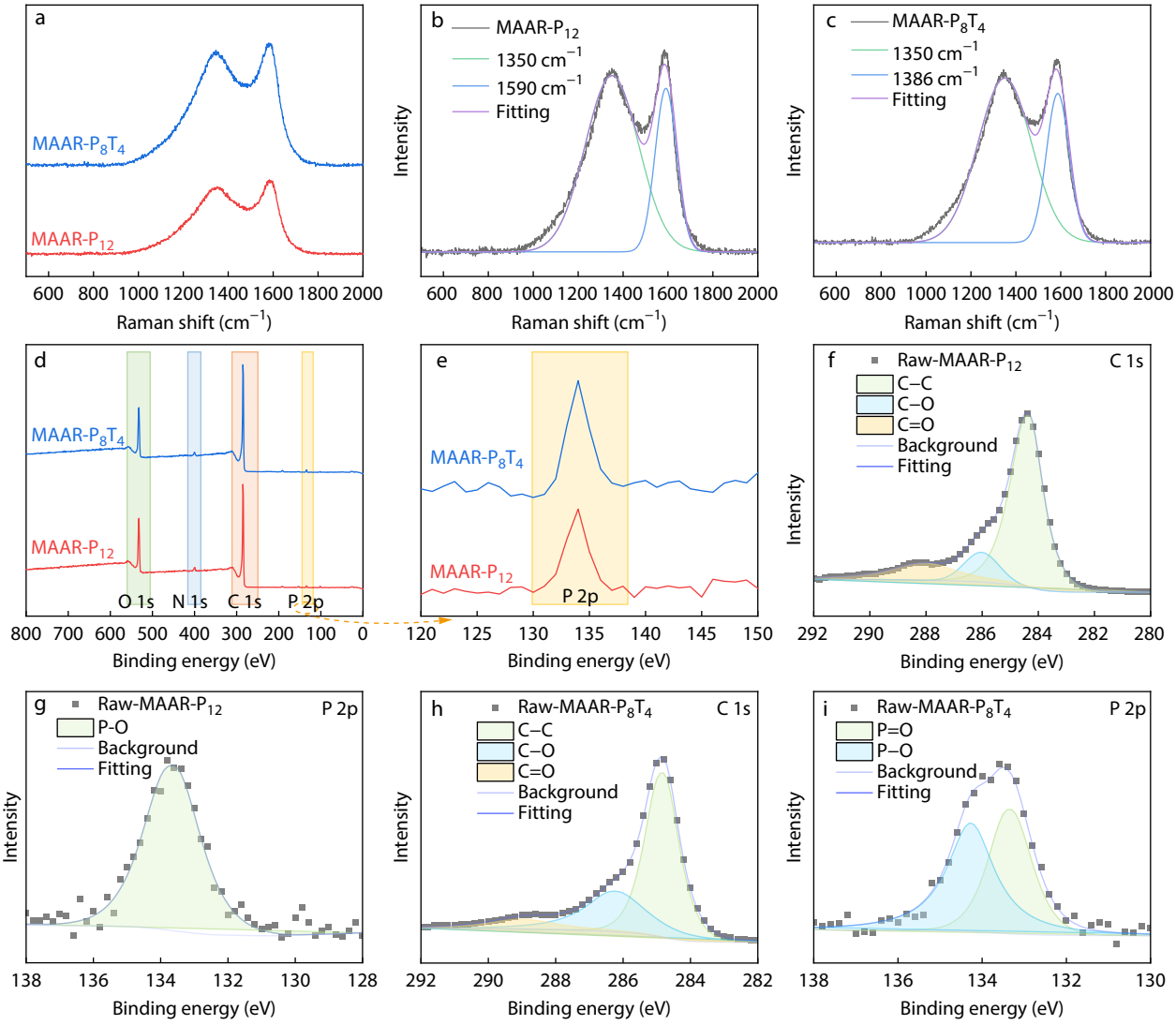

Fig. 6 (a–c) Raman spectra of MAAR-P_mT_n; (d–i) XPS spectra of MAAR-P_mT_n.

catalytic function of the flame retardant in promoting graphitic structure development during char formation.

To elucidate the flame-retardant mechanism of MAAR-P_8T_4, X-ray photoelectron spectroscopy (XPS) was employed to comparatively analyze the elemental composition of the residual char derived from MAAR-P_{12} and MAAR-P_8T_4, with the corresponding spectra presented in Figs. 6(d)–6(i).[46] As shown in Fig. 6(d), the residual chars were primarily comprised carbon (C), nitrogen (N), oxygen (O), and phosphorus (P). Notably, MAAR-P_8T_4 exhibited an enhancement in P 2p peak intensity relative to MAAR-P_{12}, indicating substantially increased phosphorus-containing substances participating in char formation. The P 2p spectra (Figs. 6g and 6i) resolved two characteristic components: the higher binding energy peak at 134.3 eV corresponding to P═O,[47] and the lower energy peak at 133.4 eV is assigned to P—O.[48] Similarly, high-resolution C 1s spectra (Figs. 6f, h) revealed three distinct components: C═O (288.4 eV),[49], C—O (286.2 eV),[50] and C—C (284.8 eV).[51] The C—C component, which encompasses both aliphatic and aromatic carbon domains, plays a critical role in enhancing oxidation resistance during combustion. Higher concentrations directly correlate with the superior thermal stability of the char.[52] Quantitative analysis demonstrated a significant increase in the C—C content from 48.16% in MAAR-P_{12} to 60.76% in MAAR-P_8T_4. This result confirms that TAEP incorporation substantially reinforces the thermo-oxidative stability of the residual char.

Finally, the gaseous pyrolyzates evolved during the thermal decomposition of the MAAR-P_mT_n coatings were comprehensively investigated using coupled thermogravimetry-Fourier transform infrared spectroscopy (TG-FTIR).[53,54] Figs. 7(a) and 7(b) presented three-dimensional FTIR spectral profiles mapping the evolution of volatile products at discrete temperature intervals for MAAR-P_{12} and MAAR-P_8T_4, respectively. Analysis of the absorption bands revealed that MAAR-P_8T_4 exhibited a lower yield of total pyrolysis products than MAAR-P_{12}. This indicates a significant synergistic effect between the flame retardants, which effectively suppressed the generation of volatiles during pyrolysis. To investigate the flame-retardant mechanism, time-resolved evolution profiles of the characteristic decomposition products were analyzed

https://doi.org/10.1007/s10118-026-3654-1

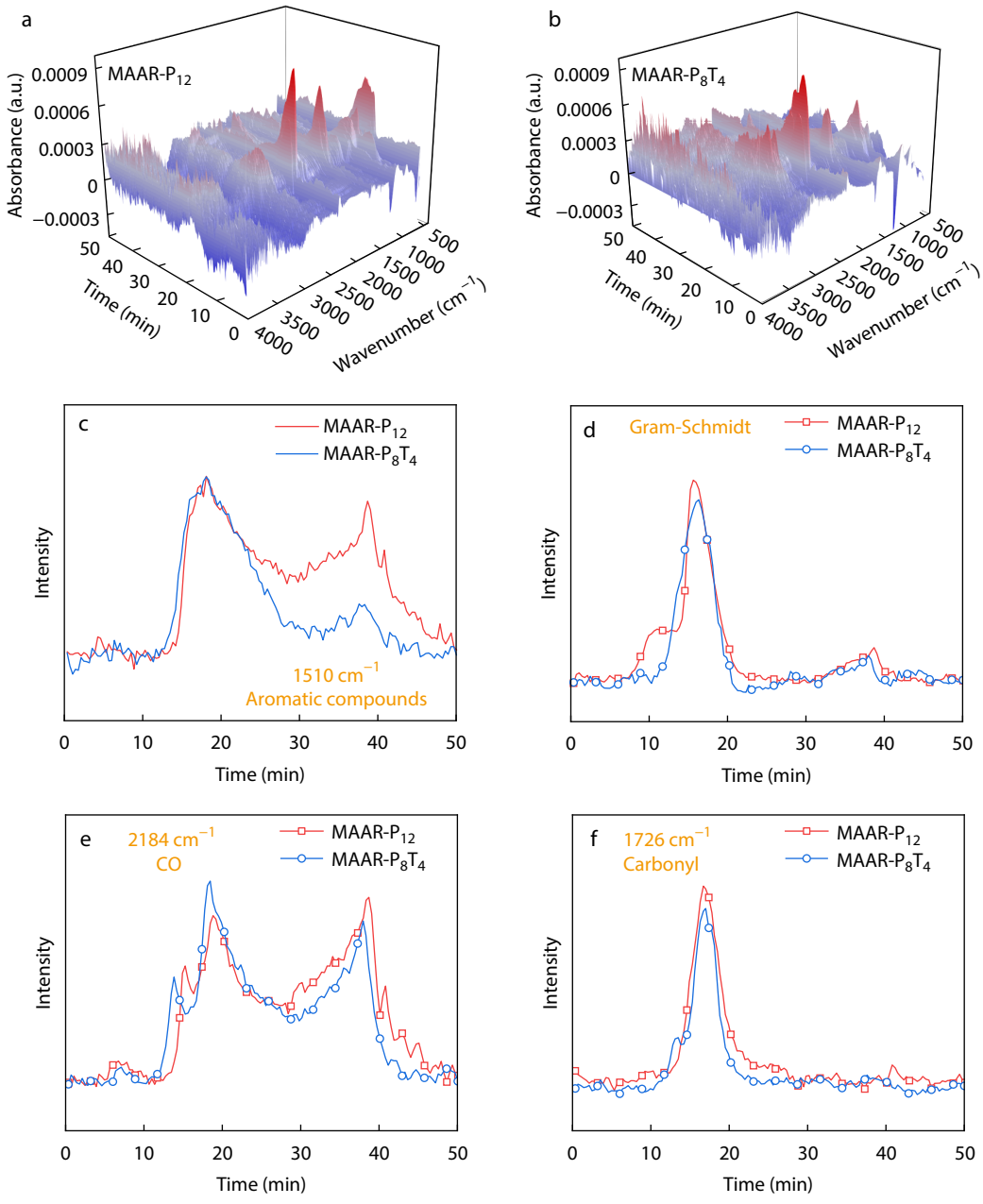

Fig. 7 (a–f) FTIR spectral analysis of gaseous degradation products from MAAR-P_mT_n.

(Figs. 7c–7f), focusing on flammable CO (2184 cm^{-1}),[55] aromatic compounds (1510 cm^{-1}),[56] and carbonyl-containing volatiles (1726 cm^{-1}).[57] All absorbance intensities were mass-normalized to enable a direct comparison. Critically, compared to MAAR-P_{12}, MAAR-P_8T_4 exhibited diminished intensity across all monitored species. This systematic suppression of combustible gases and smoke-related compounds provides evidence that the synergistic effect of PG and TAEP enhances the char-forming efficiency while impeding the fuel feed to the flame front, thereby elevating the fire safety performance of the composite.

CONCLUSIONS

Integrated analysis of the residual char and pyrolyzate evolution curves enables comprehensive elucidation of the flame-retardant mechanism in MAAR-P_8T_4. This coating demonstrates exceptional dual-phase functionality, exerting concurrent gas-phase and condensed-phase effects throughout thermal degradation.[58,59] In the gas phase, phosphorus-containing radicals liberated during pyrolysis effectively scavenge the highly reactive H• and OH• radicals *via* a quenching mechanism, thereby terminating chain combustion reactions.[60] Concurrently, non-combustible gases generate dilute fuel vapor concentrations, as quantified by TG-FTIR. Within the condensed phase, MAAR-P_8T_4 generates phosphate compounds during pyrolysis, which promote charring through cross-linking and esterification reactions and matrix dehydration. Simultaneously, these phosphates underwent esterification to form a continuous, compact char layer.

This multifunctional physical barrier achieves a 28.4% reduction in the pHRR by preventing heat feedback transfer to the polymer substrate and inhibiting the diffusion of volatiles towards the flame front. The demonstrated synergy between radical quenching, gas dilution, and barrier enhancement mechanisms collectively suppressed combustion propagation, conferring MAAR-P_8T_4 with a UL-94 V-0 rating.

Conflict of Interests

The authors declare no interest conflict.

Electronic Supplementary Information

Electronic supplementary information (ESI) is available free of charge in the online version of this article at http://doi.org/10.1007/s10118-026-3654-1.

Data Availability Statement

The data that support the findings of this study are available from the corresponding author upon reasonable request.

ACKNOWLEDGMENTS

This work was financially supported by the National Natural Science Foundation of China (Nos. 52473064 and 52321003), Cross-team for Youth Innovation in Basic Research of Qinghai Institute of Salt Lakes, Chinese Academy of Sciences (No. isIJCTD-2022-3), Key Research & Development (R&D) Plan of Anhui Province (No. 202304a05020027), and Anhui Provincial Natural Science Foundation (No. 2308085ME147). We would like to thank Dr. Yi Jin and Dr. An-Feng Shi at the Experimental Center of Engineering and Material Sciences, USTC, for their assistance with the thermophysical property analysis. This work was partially conducted at the Instruments Center for Physical Science, University of Science and Technology of China.

REFERENCES

1 Skafi, Z.; Castriotta, L. A.; Taheri, B.; Matteocci, F.; Fahland, M.; Jafarzadeh, F.; Joseph, E.; Chakraborty, A.; Singh, V.; Mottaghitalab, V.; Mivehi, L.; Brunetti, F.; Sorbello, L.; Di Carlo, A.; Brown, T. M. Flexible perovskite solar cells on polycarbonate film substrates. *Adv. Energy Mater.* **2024**, *14*, 2400912.
2 Chen, P.; Jin, J.; Zhu, Y.; Lei, Y.; Ye, X.; Dai, W.; Gu, C.; Liu, M.; Huang, X.; Wang, D. Ton-scale industrial optical polycarbonate film: combining full-color phosphorescence and various photochromic. *Adv. Sci.* **2025**, *12*, e17170.
3 Xing, D.; Lu, L.; Teh, K. S.; Wan, Z.; Xie, Y.; Tang, Y. Highly flexible and ultra-thin Ni-plated carbon-fabric/polycarbonate film for enhanced electromagnetic interference shielding. *Carbon* **2018**, *132*, 32–41.
4 Deng, P.; Chen, L.; Li, Y.; Liu, B. W.; Wang, X. L.; Wang, Y. Z. Selectively self-recyclable, highly transparent and fire-safe polycarbonate plastic enabled by thermally responsive phosphonium-phosphate. *Mater. Horiz.* **2024**, *11*, 6516–6524.
5 Kua, H. W.; Lu, Y. Environmental impacts of substituting tempered glass with polycarbonate in construction – An attributional and consequential life cycle perspective. *J. Clean. Prod.* **2016**, *137*, 910–921.
6 Wei, Y. X.; Deng, C.; Zhao, Z. Y.; Wang, Y. Z. A novel organic-inorganic hybrid SiO2@DPP for the fire retardance of polycarbonate. *Polym. Degrad. Stabil.* **2018**, *154*, 177–185.
7 Wang, X.; Ren, J.; Liu, P.; Wang, Z.; Ma, X.; Zhu, H.; Ma, Z.; Sun, Y.; Hu, Z. Study on the performance and mechanism of sulfonate phosphazene high-efficiency flame retardant polycarbonate. *J. Appl. Polym. Sci.* **2025**, *142*, e57156.
8 Yang, Y.; Kong, W.; Cai, X. Two phosphorous-containing flame retardant form a novel intumescent flame-retardant system with polycarbonate. *Polym. Degrad. Stabil.* **2016**, *134*, 136–143.
9 Wu, X.; Zhang, W.; Qin, Z.; Yang, R. Facile preparation of ladder aluminosilsesquioxanes with high flame retardancy for polycarbonate. *Polym. Degrad. Stabil.* **2024**, *222*, 110694.
10 Liu, Z.; Ma, M.; Du, K.; Wang, H.; Yan, Z.; Chen, S.; Shi, Y.; He, H.; Zhu, Y.; Wang, X. Sulfonyl-containing polycarbonate copolymer: ultra-thin flame-retardant, transparency, and high notched impact toughness. *Small* **2025**, *21*, e07493.
11 Zhang, J.; Liu, Z.; Qi, P.; Liu, J.; Sun, J.; Gu, X.; Li, H.; Zhao, J.; Zhang, S. Rapid-curing imidazole-based highly transparent protective coating for polycarbonate films with good hardness and flame retardancy. *Prog. Org. Coat.* **2024**, *189*, 108289.
12 Feng, Z.; Cai, W.; Gao, J.; Jiang, G.; Qi, L.; Li, J.; Hu, Y.; Chu, F.; Xing, W. Achieving scratch resistance and flame retardancy in transparent polycarbonate through P/N/Si synergistic coating. *Prog. Org. Coat.* **2025**, *204*, 109247.
13 Bazheva, R. C.; Kharaev, A. M.; Bazhev, A. Z.; Inarkieva, Z. I.; Beslaneeva, Z. L. Flame-resistant Copolycarbonates. *Int. Polym. Sci. Technol.* **2017**, *44*, 21–26.
14 Hou, S.; Zhang, Y. J.; Jiang, P. Phosphonium sulfonates as flame retardants for polycarbonate. *Polym. Degrad. Stabil.* **2016**, *130*, 165–172.
15 Liu, C.; Yao, Q. Design and synthesis of efficient phosphorus flame retardant for polycarbonate. *Ind. Eng. Chem. Res.* **2017**, *56*, 8789–8796.
16 Ni, P.; Fang, Y.; Qian, L.; Qiu, Y. Flame-retardant behavior of a phosphorus/silicon compound on polycarbonate. *J. Appl. Polym. Sci.* **2018**, *135*, 45815.
17 Li, X.; Cao, F.; Peng, M.; Ai, J.; Zhang, Y.; Ding, C.; Ye, N.; Chen, P.; Zhao, H. Recent progress in flame retardant technology for polycarbonate: advancing from halogenated to halogen-free and PFAS-free solutions. *J. Appl. Polym. Sci.* **2025**, *143*, e58149.
18 Sai, T.; Ran, S.; Guo, Z.; Yan, H.; Zhang, Y.; Wang, H.; Song, P.; Fang, Z. Transparent, highly thermostable and flame retardant polycarbonate enabled by rod-like phosphorous-containing metal complex aggregates. *Chem. Eng. J.* **2021**, *409*, 128223.
19 Wang, Z.; Qiu, Y.; Liu, A.; Tang, W.; Xi, W.; Wang, J.; Gao, L. B.; Qian, L. Micro-crosslinking of phosphaphenanthrene/siloxane molecule initiate aggregation flame retardant and toughening enhancement effects on its polycarbonate composite. *Chem. Eng. J.* **2023**, *466*, 143169.
20 Yin, Z. Z.; Ma, J. M.; Zhao, B.; Yan, H.; Zhang, C. Y. PVA-based hydrogen-bonded supramolecular adhesive with core–shell nanoarchitectures for multifunctional and sustainable applications. *J. Adv. Res.* **2025**.
21 Liu, C.; Huang, T. T.; Yang, K.; Zhang, C. Y.; Yan, H.; Zhao, B. One-step construction of a phosphazene-based hybrid coating for flame-retardant, antimicrobial, and hydrophobic viscose fabric. *Surf. Coat. Technol.* **2025**, *516*, 132769.
22 Liu, N.; Liu, Q.; Lozano, J. S.; Shu, L.; Zhang, L.; Zhu, J.; Deng, Z.; Satoh, K. Global burning rate of square fire arrays: experimental correlation and interpretation. *Proc. Combust. Inst.* **2009**, *32*, 2519–2526.

Graphical Abstract

Transparent UV-cured Phosphorus/Nitrogen Hybrid Coating for Simultaneously Enhancing Flame Retardancy and Surface Hardness of Polycarbonate

Jing Gao, Liang Chen, Liang-Yuan Qi, Su-Hong Li, Yuan Hu, Xin Wang, Lian-Min Ji, Ying-Jian Wang, and Wei-Yi Xing

University of Science and Technology of China; Beijing University of Posts and Telecommunications; Qinghai Institute of Salt Lakes, Chinese Academy of Sciences

Using UV curing technology, transparent flame-retardant coatings with an average transmittance exceeding 90% were formed on the surface of polycarbonate films. MAAR-P_8T_4 enables 0.5 mm thick polycarbonate film to achieve a UL-94 vertical burning rating of V-0.

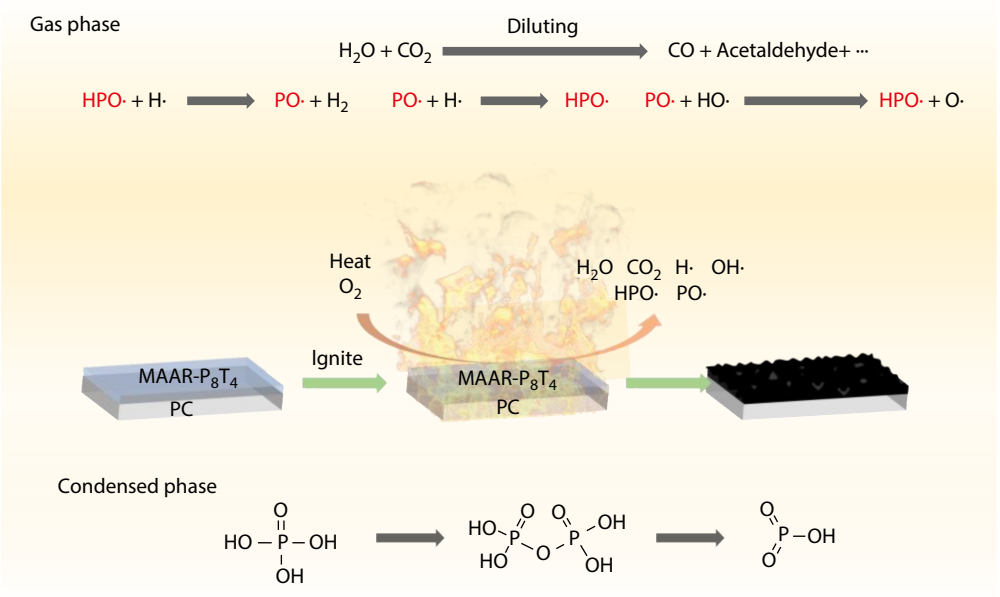

Chinese J. Polym. Sci., 2026 *https://doi.org/10.1007/s10118-026-3654-1*

23 Qian, Z.; Zou, B.; Xiao, Y.; Qiu, S.; Xu, Z.; Yang, Y.; Jiang, G.; Zhang, Z.; Song, L.; Hu, Y. Targeted modification of black phosphorus by MIL-53(Al) inspired by "Cannikin's Law" to achieve high thermal stability of flame retardant polycarbonate at ultra-low additions. *Compos. Part B Eng.* **2022**, *238*, 109943.
24 Hilt, F.; Gherardi, N.; Duday, D.; Berné, A.; Choquet, P. Efficient flame retardant thin films synthesized by atmospheric pressure PECVD through the high co-deposition rate of hexamethyldisiloxane and triethylphosphate on polycarbonate and polyamide-6 substrates. *ACS Appl. Mater. Interfaces* **2016**, *8*, 12422–12433.
25 Li, Y.; Niu, H. X.; Jiang, H. R.; Ma, C.; Yan, Y.; Shi, H. J.; Zhou, K. S.; Hu, Y.; Wang, X. Cardanol-derived phosphorus-containing acrylates as UV-curable, highly transparent and flame retardant coatings for polycarbonate. *Ind. Crops Prod.* **2025**, *233*, 121386.
26 Zhang, W.; Feng, Z.; Chen, Z.; He, L.; Qi, L.; Hu, Y.; Gui, Z.; Xing, W. Phosphorus-nitrogen synergistic transparent UV-curable coatings to enhance the flame retardancy of polycarbonate. *Polym. Degrad. Stabil.* **2024**, *225*, 110782.
27 Qi, L.; Qiu, S.; Xi, J.; Yu, B.; Hu, Y.; Xing, W. Construction of superhydrophobic, highly effective flame retardant coating for cotton fabric with superior washability and abrasion resistance. *J. Colloid Interface Sci.* **2022**, *607*, 2019–2028.
28 Qi, L.; Chen, L.; Cai, W.; Wang, C.; Wang, B.; Hu, Y.; Xing, W. Intelligent polyester fabric with fire safety for personal temperature management. *Chem. Eng. J.* **2023**, *475*, 146272.
29 Qi, L.; Wang, B.; Zhang, W.; Yu, B.; Zhou, M.; Hu, Y.; Xing, W. Durable flame retardant and dip-resistant coating of polyester fabrics by plasma surface treatment and UV-curing. *Prog. Org. Coat.* **2022**, *172*, 107066.
30 Beyler-Çiğil, A. Designing superhydrophobic and flame retardant photo-cured hybrid coatings. *Prog. Org. Coat.* **2020**, *148*, 105850.
31 Liang, B.; Bai, Z.; Zhou, H.; Cui, J.; Xu, X.; Zhu, Y.; Wang, H. Multifunctional photocurable liquid-like amphiphobic coating with anti-scaling and anti-corrosion performance. *Prog. Org. Coat.* **2025**, *209*, 109562.
32 Qiao, S.; Shi, Z.; Zhang, Y.; Zhang, G.; Huang, Z.; He, A.; Chen, M.; Ke, G.; Yuan, J.; Chen, S.; Chen, F. Colorful polyester with high-efficiency flame retardant and anti-dripping properties. *Chem. Eng. J.* **2025**, *521*, 166544.

33 Chen, S.; Li, J.; Yuan, Y.; Fu, Z.; Ma, D.; Zhang, L.; Wang, G.; Fang, D. Zinc hydroxystannate coated by polyphosphazene to improve the fire safety and suppress the smoke of epoxy resin. *Prog. Org. Coat.* **2024**, *186*, 108041.

34 Shen, Q.; Yu, B.; Chen, D.; Zhang, F.; Wang, L.; Ma, Y.; Yang, W. Novel furfuryl-based phosphaphenanthrene containing N/P flame retardant: towards epoxy resin with excellent flame retardancy, enhanced toughness and low dielectric constant. *Chem. Eng. J.* **2025**, *519*, 165034.

35 Wang, G.; Ran, F.; Hui, X.; Fang, D.; Li, J.; Ma, D.; Zhang, X.; Fu, Z.; Mukhamediev, M. Ultrasonic co-precipitation synthesis of phosphonitrile-modified calcium hydroxystannate hybrids for epoxy composites: synergistic reduction in heat release and toxic gas emission. *Colloids Surf. Physicochem. Eng. Aspects* **2025**, *726*, 138034.

36 Chen, Z.; Bi, X.; Shi, Y.; Xue, D.; Li, T.; Zhang, B.; Gao, Z.; Zhao, T. Dual covalent crosslinking strategy to fabricate flame-retardant, hydrophobic, high-strength and breathable fabric. *Chem. Eng. J.* **2025**, *520*, 165781.

37 Dong, F.; Wang, Y.; Wang, S.; Shaghaleh, H.; Sun, P.; Huang, X.; Xu, X.; Wang, S.; Liu, H. Flame-retarded polyurethane foam conferred by a bio-based nitrogen-phosphorus-containing flame retardant. *React. Funct. Polym.* **2021**, *168*, 105057.

38 Kim, T. Y.; Park, J. H.; Kim, O. Y.; Hwang, S. H. The effect of chemically modified expandable graphite on flame-retardant properties of waterborne intumescent flame-retardant coating. *J. Ind. Eng. Chem.* **2025**, *149*, 366–373.

39 Wang, J.; Guo, Y.; Zhao, S.; Huang, R. Y.; Kong, X. J. A novel intumescent flame retardant imparts high flame retardancy to epoxy resin. *Polym. Adv. Technol.* **2020**, *31*, 932–940.

40 Huang, Z.; Li, S.; Tsai, L. C.; Jiang, T.; Ma, N.; Tsai, F. C. Flame retardant polypropylene with a single molecule intumescent flame retardant based on chitosan. *Mater. Today Commun.* **2022**, *33*, 104689.

41 Feng, C.; Liang, M.; Jiang, J.; Huang, J.; Liu, H. Flame retardant properties and mechanism of an efficient intumescent flame retardant PLA composites. *Polym. Adv. Technol.* **2016**, *27*, 693–700.

42 Yuan, J.; Wang, H.; Wang, Y.; Ma, Y.; Zhu, Z.; Lin, X. A novel highly efficient intumescent flame-retardant polypropylene: Thermal degradation, flame retardance and mechanism. *J. Polym. Res.* **2022**, *29*, 205.

43 Zhang, D.; Williams, B. L.; Becher, E. M.; Shrestha, S. B.; Nasir, Z.; Lofink, B. J.; Santos, V. H.; Patel, H.; Peng, X.; Sun, L. Flame retardant and hydrophobic cotton fabrics from intumescent coatings. *Adv. Compos. Hybrid Mater.* **2018**, *1*, 177–184.

44 Lee, J.; Park, K.; Oh, S. M.; Kim, B. S.; Kang, H. I.; Baeck, S. H.; Shim, S. E.; Qian, Y. Facile preparation of heptazine-covered Fe2O3 and its synergistic effect on the enhanced flame retardance of silicone rubber composite. *Compos. Commun.* **2024**, *51*, 102104.

45 Wang, Z.; Gong, G.; Gao, L.; Cui, W.; Wang, Y. Preparation and performance of intumescent water-based coatings with both thermal insulation and flame retardant functions. *Chem. Eng. J.* **2024**, *480*, 148165.

46 Chen, B.; Wu, D.; Wang, T.; Liu, Q.; Jia, D. Porous carbon generation by burning starch-based intumescent flame retardants for supercapacitors. *Chem. Eng. J.* **2024**, *486*, 150353.

47 Qi, L.; Cai, W.; Cui, T.; Li, J.; Song, L.; Gui, Z.; Fei, B.; Zhu, J.; Hu, Y.; Xing, W. Anisotropic radiative cooling dynamics enabling efficient thermal hazard mitigation *via* hierarchically engineered thermal diodes. *Adv. Funct. Mater.* **2025**, *36*, e08101.

48 Li, X.; Zhao, Z.; Wang, Y.; Yan, H.; Zhang, X.; Xu, B. Highly efficient flame retardant, flexible, and strong adhesive intumescent coating on polypropylene using hyperbranched polyamide. *Chem. Eng. J.* **2017**, *324*, 237–250.

49 Ma, T.; Zhou, Q.; Li, L.; Pan, M.; Guo, C.; Mei, C. Nacre-inspired intumescent flame retardant bridging network for intelligent fire warning and prevention. *Chem. Eng. J.* **2023**, *468*, 143786.

50 Deng, X.; Li, C.; Sun, X.; Wang, C.; Liu, B.; Li, Y.; Yang, H. Flame-retardant wood-based composite phase change materials based on PDMS/expanded graphite coating for efficient solar-to-thermal energy storage. *ApEn* **2024**, *368*, 123454.

51 Tang, W.; Qian, L.; Prolongo, S. G.; Qiu, Y.; Wang, D. Y. Macromolecular piperazine/aluminum phosphate hybrid and its efficient intumescent flame retardant/thermal conductive polypropylene. *Chem. Eng. J.* **2024**, *495*, 153162.

52 Wu, W.-S.; Ni, Y.-P.; Chen, L.; Fu, T.; Wang, X.-L.; Wang, Y.-Z. Trinity effect of potassium sulfonate-benzimidozale towards self-intumescent flame-retarded polyester with low fire hazards. *Chem. Eng. J.* **2022**, *429*, 132121.

53 Jian, R. K.; Ai, Y. F.; Xia, L.; Zhao, L. J.; Zhao, H. B. Single component phosphamide-based intumescent flame retardant with potential reactivity towards low flammability and smoke epoxy resins. *J. Hazard. Mater.* **2019**, *371*, 529–539.

54 Li, Y.; Su, Q.; Leng, Y.; Sun, P.; Han, X.; Xu, M.; Li, X.; Li, B. Silane-modified magnesium oxide synergized with diphenyl chlorophosphate for high thermal conductivity and flame-retardant epoxy composites. *Compos. Commun.* **2025**, *60*, 102617.

55 Qi, L.; Cai, W.; Cui, T.; Chen, L.; Gao, J.; Wang, W.; Rahman, M. Z.; Gui, Z.; Fei, B.; Hu, Y.; Xing, W. Enhanced radiative cooling and flame retardancy through phosphate-linked hollow metal-organic framework spheres. *Chem. Eng. J.* **2025**, *507*, 160469.

56 Ye, X.; Zhan, C.; Sai, T.; Wang, B.; Li, J.; Zhang, C.; Wang, Y.; Guo, Z.; Huo, S. Flame-retardant and UV-resistant polycarbonate composites with well-preserved mechanical properties enabled by silsesquioxane/sulfonate-functionalized nano carbon black. *Compos. Commun.* **2025**, *56*, 102407.

57 Chen, S.; Li, X.; Li, Y.; Sun, J. Intumescent flame-retardant and self-healing superhydrophobic coatings on cotton fabric. *ACS Nano* **2015**, *9*, 4070–4076.

58 Cai, G.; Liu, A.; He, Y.; Hu, Z.; Bian, J.; Zhang, Y.; Zhang, H.; Wang, M. Preparation and performance analysis of a novel zirconium-doped silicone resin modified epoxy resin-based intumescent flame-retardant and thermal-insulating coating. *Chem. Eng. J.* **2025**, *520*, 165996.

59 Zheng, S.; Shi, S.; Zeng, K.; Zhou, X.; Zhou, L.; Rao, W.; Yu, C. A compound containing phosphorus-rich arcuate structure towards improving fire safety and toughness, and maintaining transparency of epoxy resins. *Compos. Commun.* **2025**, *56*, 102386.

60 Yang, S.; Zhang, J.; Liu, G.; Wang, R.; Zhang, X. Poly-D-lactic acid (PDLA) and schiff base dual modifications of the cyclodextrin-Based hierarchical fire retardants towards fire safe and UV-resistant poly-L-lactic acid (PLLA). *Compos. Commun.* **2025**, *54*, 102257.

https://doi.org/10.1007/s10118-026-3654-1